

Published in final edited form as:

Inorg Chem. 2013 December 2; 52(23): . doi:10.1021/ic402121j.

Photochemical Oxidation of a Manganese(III) Complex with Oxygen and Toluene Derivatives to Form a Manganese(V)-Oxo Complex

 Jieun Jung[†], Kei Ohkubo[†], Katharine A. Prokop-Prigge[‡], Heather M. Neu[‡], David P. Goldberg^{*,‡}, and Shunichi Fukuzumi^{*,†,§}
[†]Department of Material and Life Science, Graduate School of Engineering, ALCA, Japan Science and Technology Agency, Osaka University, Suita, Osaka 565-0871, Japan

[‡]Department of Chemistry, The Johns Hopkins University, Baltimore, Maryland 21218, United States

[§]Department of Bioinspired Science, Ewha Womans University, Seoul 120-750, Korea

Abstract

Visible light photoirradiation of an oxygen-saturated benzonitrile solution of a manganese(III) corrolazine complex [(TBP₈Cz)Mn^{III} (**1**): [TBP₈Cz = octakis(*p*-*tert*-butylphenyl)corrolazinato³⁻] in the presence of toluene derivatives resulted in formation of the manganese(V)-oxo complex [(TBP₈Cz)Mn^V(O)]. The photochemical oxidation of (TBP₈Cz)Mn^{III} with O₂ and hexamethylbenzene (HMB) led to the isosbestic conversion of **1** to (TBP₈Cz)Mn^V(O), accompanied by the selective oxidation of HMB to pentamethylbenzyl alcohol (87%). The formation rate of (TBP₈Cz)Mn^V(O) increased with methyl group substitution, from toluene, *p*-xylene, mesitylene, durene, pentamethylbenzene, up to hexamethylbenzene. Deuterium kinetic isotope effects (KIEs) were observed for toluene (KIE = 5.4) and mesitylene (KIE = 5.3). Femtosecond laser flash photolysis of (TBP₈Cz)Mn^{III} revealed the formation of a triplet excited state, which was rapidly converted to a triplet excited state. The triplet excited state was shown to be the key, activated state that reacts with O₂ via a diffusion-limited rate constant. The data allow for a mechanism to be proposed in which the triplet excited state reacts with O₂ to give the putative (TBP₈Cz)Mn^{IV}(O₂^{•-}), which then abstracts a hydrogen atom from the toluene derivatives in the rate-determining step. The mechanism of hydrogen abstraction is discussed by comparison of the reactivity with the hydrogen abstraction from the same toluene derivatives by cumylperoxyl radical. Taken together, the data suggest a new catalytic method is accessible for the selective oxidation of C-H bonds with O₂ and light, and the first evidence for catalytic oxidation of C-H bonds was obtained with 10-methyl-9,10-dihydroacridine as a substrate.

INTRODUCTION

High-valent metal-oxo species are key oxidizing intermediates in a variety of biological oxidation reactions mediated by heme and non-heme metalloenzymes involved in respiration, metabolism, and photosynthesis.¹⁻⁴ Synthetic high-valent metal-oxo complexes

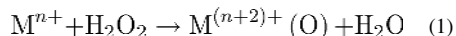
* To whom correspondence should be addressed. fukuzumi@chem.eng.osaka-u.ac.jp, dp@jhu.edu.

ASSOCIATED CONTENT

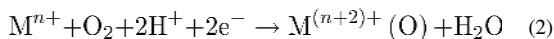
Supporting Information

UV-vis spectra (Figure S1, S2, S3 and S13), GC charts (Figure S4), calibration plots for GC measurements (Figure S5), kinetic plots (Figures S6, S7, S8, S9, S10, S11 and S12), phosphorescence spectra (Figures S14), and yields of the products (Table S1). This material is available free of charge via the Internet at <http://pubs.acs.org>.

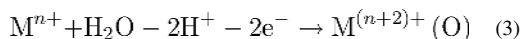
($M^{(n+2)+}(O)$) are usually formed by reactions of metal complexes (M^{n+}) with two-electron oxidants such as iodoylarenes, peroxy acids, and H_2O_2 [eqn (1)].⁵⁻¹⁶ However, enzymes such as cytochrome



P450 use dioxygen (O_2) together with the addition of two electrons and two protons, which is equivalent to H_2O_2 , to generate a high-valent metal-oxo species [eqn (2)].^{1,2} On the other hand,



high-valent manganese-oxo species are implicated in the water oxidation mechanism of Photosystem II, and may involve the formal two-electron oxidation of a H_2O molecule by a tetranuclear manganese complex to give high-valent Mn(O) intermediates.^{4,5} Synthetic high-valent metal-oxo complexes have also been reported to be formed by two-electron oxidation of metal complexes with H_2O as the oxygen source [eqn (3)].¹⁷⁻²³



There have been comparatively few reports on the formation of discrete, high-valent metal-oxo complexes using O_2 .²⁴⁻²⁶ The activation of O_2 and stabilization of high-valent metal-oxo species is challenging to carry out in a single ligand environment. Porphyrinoid ligands, and in particular corroles and corrolazines (Czs), are designed to stabilize high-valent species including high-valent metal-oxo complexes, and there are examples of $Cr^V(O)$ corroles generated from O_2 .²⁷ It has recently been reported that the oxidation of a Mn^{III} corrolazine complex with O_2 in cyclohexane or toluene as solvent under visible light irradiation leads to the quantitative production of a well-characterized, isolable $Mn^V(O)$ complex.²⁸ Relatively short-lived metal-oxo species have been generated by photo-initiated homolytic axial ligand cleavage reactions with metalloporphyrins, as well as photochemical splitting of metalloporphyrin μ -oxo dimers.^{29,30} However, to our knowledge the former photo-initiated reaction involving $Mn^{III}(Cz)$ is the first example of the production of a well-defined $Mn^V(O)$ species from O_2 .

In the former study, the combined data suggested a mechanism for the generation of $Mn^V(O)(Cz)$ that involved solvent-assisted autoxidation, in which the solvent (cyclohexane or toluene) served as a sacrificial reductant for the activation and cleavage of a putative photactivated Mn- O_2 intermediate. The nature of the photoexcited state, and the product(s) of solvent oxidation were not identified in this study. The proposed mechanism suggested that, perhaps under conditions involving an inert solvent, the controlled oxidation of substrates such as toluene derivatives could be mediated by $Mn^{III}(Cz)/O_2$ /light.

We report herein the use of benzonitrile (PhCN) as an inert solvent for the reaction of the Mn^{III} complex [(TBP₈Cz)Mn^{III}: TBP₈Cz = octakis(*p*-*tert*-butylphenyl)corrolazinato³⁻] with O_2 under visible light irradiation. The conversion of (TBP₈Cz)Mn^{III} to (TBP₈Cz)Mn^V(O) does not occur in PhCN in the absence of a proton/electron source, but with the addition of a series of toluene derivatives as substrates the smooth production of the $Mn^V(O)$ complex is observed. The concomitant oxidation of the toluene derivatives occurs with high selectivity and efficiency, leading to monohydroxylation of a benzylic position. Femtosecond laser flash photolysis (LFP) measurements resulted in the spectroscopic observation of a short-lived, O_2 -reactive (TBP₈Cz)Mn^{III} excited state. The LFP experiments, together with product analyses and kinetic measurements, including kinetic

deuterium isotope effects, provide valuable insights into the mechanism of generation of the $\text{Mn}^{\text{V}}(\text{O})$ complex by the photochemical oxidation of the Mn^{III} complex using O_2 as an oxygen source and toluene derivatives as the source of protons and electrons.

EXPERIMENTAL SECTION

Materials

The starting material $(\text{TBP}_8\text{Cz})\text{Mn}^{\text{III}}$ was synthesized according to published procedures.³¹ The commercially available reagents (*p*-xylene, mesitylene, durene, pentamethylbenzene, and hexamethylbenzene) were purchased with the best available purity and used without further purification. Toluene and benzonitrile (PhCN) were dried according to literature procedures³² and distilled under Ar prior to use. The reagents 2,3,4,5,6-pentamethylbenzyl alcohol and pentamethylbenzaldehyde were also purchased with the best available purity and used without further purification from Wako Pure Chemical Industries, Ltd. and Tokyo Kasei Co., Ltd, respectively. Di-*tert*-butylperoxide was purchased from Nacalai Tesque Co., Ltd. and purified by chromatography through alumina, which removes traces of the hydroperoxide. 10-Methyl-9,10-dihydroacridine (AcrH_2) was prepared from 10-methylacridinium perchlorate ($\text{AcrH}^+\text{ClO}_4^-$) by reduction with NaBH_4 in methanol and purified by recrystallization from ethanol.³³ Cumene was purchased from Tokyo Kasei Co., Ltd. and also purified by chromatography through alumina. Deuterated toluene and mesitylene were purchased from Cambridge Isotopes in the highest purity and used as received.

Product Analysis

A PhCN solution of $(\text{TBP}_8\text{Cz})\text{Mn}^{\text{III}}$ (5.0×10^{-4} M) was added with a microsyringe into an O_2 -saturated PhCN solution containing hexamethylbenzene (2.0×10^{-2} M) as a substrate in a quartz cell. A rather large concentration of $(\text{TBP}_8\text{Cz})\text{Mn}^{\text{III}}$ was employed to obtain detectable amounts of products by GC-MS. The mixture of the reaction was filled with O_2 and then irradiated for 24 h at room temperature, when the solution changed from the green-brown color indicative of $(\text{TBP}_8\text{Cz})\text{Mn}^{\text{III}}$ to the bright-green color of $(\text{TBP}_8\text{Cz})\text{Mn}^{\text{V}}(\text{O})$. Complete conversion of $(\text{TBP}_8\text{Cz})\text{Mn}^{\text{III}}$ to $(\text{TBP}_8\text{Cz})\text{Mn}^{\text{V}}(\text{O})$ was confirmed by UV-vis spectroscopy by sampling an aliquot of the reaction mixture. An aliquot was removed and injected directly into the GC-MS for analysis. All peaks of interest were identified by comparison of retention times and co-injection with authentic samples. Compounds were quantified by comparison against a known amount of detected products using a calibration curve consisting of a plot of mole versus area. Calibration curves were prepared by using concentrations in the same range as that observed in the actual reaction mixtures. Mass spectra were recorded with a JEOL JMS-700T Tandem MS station, and the GC-MS analyses were carried out by using a Shimadzu GCMS-QP2000 gas chromatograph mass spectrometer. GC-MS conditions in these experiments were performed as follows: an initial oven temperature of 60 °C was held for 1 min and then raised 30 °C min^{-1} for 7.3 min until a temperature of 280 °C was reached, which was then held for further 10 min. This experiment was repeated three times, exhibiting error in yields within 10%.

Spectral and Kinetic Measurements

The photochemical oxidations of $(\text{TBP}_8\text{Cz})\text{Mn}^{\text{III}}$ (7.6×10^{-6} M) with excess O_2 were examined by monitoring UV-vis spectral changes in the presence of a large excess of toluene derivatives (2.0×10^{-2} to 9.4 M) at 298 K using a Hewlett-Packard HP8453 diode array spectrophotometer under continuous irradiation of white light from a Shimadzu RF-5300PC fluorescence spectrophotometer at the same time. Typically, an aerated PhCN solution of $(\text{TBP}_8\text{Cz})\text{Mn}^{\text{III}}$ was added with a microsyringe to an aerated PhCN solution containing the toluene derivatives in a quartz cell (total vol. 2.0 mL). Rates of oxidation

reaction of $(\text{TBP}_8\text{Cz})\text{Mn}^{\text{III}}$ to produce $(\text{TBP}_8\text{Cz})\text{Mn}^{\text{V}}(\text{O})$ were monitored by the decrease in the absorption band due to $(\text{TBP}_8\text{Cz})\text{Mn}^{\text{III}}$ ($\lambda_{\text{max}} = 695 \text{ nm}$, $\epsilon_{\text{max}} = 3.51 \times 10^4 \text{ M}^{-1} \text{ cm}^{-1}$). The concentration of toluene derivatives were maintained in large excess as compared to $[(\text{TBP}_8\text{Cz})\text{Mn}^{\text{III}}]$ for all kinetic measurements. The limiting concentration of O_2 in PhCN solution was prepared by a mixed gas flow of O_2 and N_2 . The mixed gas was controlled by using a gas mixer (Kofloc GB-3C, KOJIMA Instrument Inc.), which can mix two or more gases at a certain pressure and flow rate.

Quantum Yield Determination

A standard actinometer (potassium ferrioxalate)³⁴ was used for the quantum yield determination of the photochemical oxidation of $(\text{TBP}_8\text{Cz})\text{Mn}^{\text{III}}$ with O_2 and toluene derivatives in O_2 -saturated PhCN. Typically, a square quartz cuvette (10 mm i.d.), which contained an O_2 -saturated PhCN solution (2.0 mL) of $(\text{TBP}_8\text{Cz})\text{Mn}^{\text{III}}$ ($7.6 \times 10^{-6} \text{ M}$) and a toluene derivative was irradiated with monochromatic light of $\lambda = 450 \text{ nm}$ from a Shimadzu RF-5300PC fluorescence spectrophotometer. Under the conditions of actinometry experiments, the actinometer and $(\text{TBP}_8\text{Cz})\text{Mn}^{\text{III}}$ absorbed essentially all of the incident light at $\lambda = 450 \text{ nm}$. The light intensity of monochromatized light at $\lambda = 450 \text{ nm}$ was determined to be $3.7 \times 10^{-8} \text{ einstein s}^{-1}$. The quantum yields were determined by monitoring the disappearance of absorbance at 695 nm due to $(\text{TBP}_8\text{Cz})\text{Mn}^{\text{III}}$.

Photocatalytic Activity Measurements

The photocatalytic reactivity of $(\text{TBP}_8\text{Cz})\text{Mn}^{\text{III}}$ ($1.7 \times 10^{-4} \text{ M}$) with excess of O_2 was examined by monitoring the UV-vis spectral changes in the presence of a large excess of AcrH_2 (0.2 M) in a quartz cell (optical path length 1 mm) using a Xe lamp (500 W) for irradiation through a transmitting glass filter ($\lambda > 480 \text{ nm}$) at room temperature. In a typical experiment, $(\text{TBP}_8\text{Cz})\text{Mn}^{\text{III}}$ ($1.7 \times 10^{-4} \text{ M}$) was dissolved in PhCN (0.5 mL) containing excess AcrH_2 (0.2 M). The solution was purged with O_2 gas for 10 min in the quartz cell, and then the reaction was initiated by irradiating the solution with a Xe lamp (500 W) transmitting through a glass filter ($\lambda > 480 \text{ nm}$). The UV-vis spectra of the solution were measured using a Hewlett-Packard HP8453 diode array spectrophotometer every 1 h. The amount of 10-methyl-(9,10H)-acridinone ($\text{Acr}=\text{O}$) produced was quantified by an increase in the absorption band due to $\text{Acr}=\text{O}$ ($\lambda = 402 \text{ nm}$, $\epsilon_{\text{max}} = 8.6 \times 10^3 \text{ M}^{-1} \text{ cm}^{-1}$ in PhCN).

Femtosecond Laser Flash Photolysis Measurements

Measurements of transient absorption spectra in the oxidation reaction of $(\text{TBP}_8\text{Cz})\text{Mn}^{\text{III}}$ were performed according to the following procedures. An O_2 - or N_2 -saturated PhCN solution containing $(\text{TBP}_8\text{Cz})\text{Mn}^{\text{III}}$ ($6.8 \times 10^{-5} \text{ M}$) was excited using an ultrafast source, Integra-C (Quantronix Corp.), an optical parametric amplifier, TOPAS (Light Conversion Ltd.), and a commercially available optical detection system, Helios provided by Ultrafast Systems LLC. The source for the pump and probe pulses were derived from the fundamental output of Integra-C ($\lambda = 786 \text{ nm}$, 2 mJ/pulse and fwhm = 130 fs) at a repetition rate of 1 kHz. 75% of the fundamental output of the laser was introduced into a second harmonic generation (SHG) unit: Apollo (Ultrafast Systems) for excitation light generation at $\lambda = 393 \text{ nm}$, while the rest of the output was used for white light generation. The laser pulse was focused on a sapphire plate of 3 mm thickness and then white light continuum covering the visible region from $\lambda = 410 \text{ nm}$ to 800 nm was generated via self-phase modulation. A variable neutral density filter, an optical aperture, and a pair of polarizer were inserted in the path in order to generate stable white light continuum. Prior to generating the probe continuum, the laser pulse was fed to a delay line that provides an experimental time window of 3.2 ns with a maximum step resolution of 7 fs. In our experiments, a wavelength at $\lambda = 393 \text{ nm}$ of SHG output was irradiated at the sample cell with a spot size of 1 mm

diameter where it was merged with the white probe pulse in a close angle ($< 10^\circ$). The probe beam after passing through the 2 mm sample cell was focused on a fiber optic cable that was connected to a CMOS spectrograph for recording the time-resolved spectra ($\lambda = 410\text{-}800\text{ nm}$). Typically, 1500 excitation pulses were averaged for 3 seconds to obtain the transient spectrum at a set delay time. Kinetic traces at appropriate wavelengths were assembled from the time-resolved spectral data. The decay rate of the triplet (5T_1) obeyed the first-order kinetics given by eqn (4) where A_1 and A_2 are pre-

$$\Delta\text{Abs} = A_1 \exp(-k_1 t) + A_2 \quad (4)$$

exponential factors for the absorbance changes and k_1 is the rate constant of the decay of the triplet (5T_1) after irradiation. The slower decay rate of the triplet (7T_1) also obeyed the first-order kinetics given by eqn (5), where A_3 is the final absorbance at 774 nm and k_2 is the rate

$$\Delta\text{Abs} = A_1 \exp(-k_1 t) + A_2 \exp(-k_2 t) + A_3 \quad (5)$$

constant of the decay of 7T_1 . All measurements were conducted at room temperature, 298 K.

EPR Measurements

Photoirradiation of an oxygen-saturated PhCN solution containing di-*tert*-butylperoxide (1.0 M) and cumene (1.0 M) with a 1000 W mercury lamp (Ushio-USH1005D) through an aqueous filter resulted in formation of cumylperoxyl radical ($g = 2.0156$).³⁵ The EPR spectra were measured with a JEOL X-band spectrometer (JES-RE1XE). The ESR spectra were recorded under non-saturating microwave power conditions. The magnitude of modulation was chosen to optimize the resolution and the signal-to-noise (S/N) ratio of the observed spectra. The g value was calibrated by using a Mn^{2+} marker. Upon cutting off the light irradiated through a window directly, the decay of the EPR intensity was recorded with time. The decay rates were accelerated by the presence of toluene derivatives, indicating hydrogen atom transfer occurred. Rates of hydrogen atom transfer from toluene derivatives to cumylperoxyl radical were monitored by measuring the decay of the EPR signal in the presence of various concentrations of toluene derivatives in propionitrile at -80°C . Pseudo-first-order rate constants were determined by a least-squares curve fitting procedure. The first-order plots of $\ln(I - I_\infty)$ vs time (I and I_∞ are the EPR intensity at time t and the final intensity, respectively) were linear for three or more half-lives with the correlation coefficient, $\rho > 0.99$. Plot of the pseudo-first-order rate constants against the substrate concentrations gave linear lines.

RESULTS AND DISCUSSION

Photochemical Oxidation of $(\text{TBP}_8\text{Cz})\text{Mn}^{\text{III}}$ with O_2 and Toluene Derivatives

The photochemical generation of a $\text{Mn}^{\text{V}}(\text{O})$ complex using O_2 as an oxygen source was performed by photoirradiation of an aerated PhCN solution containing a Mn^{III} complex [$(\text{TBP}_8\text{Cz})\text{Mn}^{\text{III}}$] and toluene derivatives (Scheme 1). Monitoring this reaction by UV-vis spectroscopy revealed the transformation of $(\text{TBP}_8\text{Cz})\text{Mn}^{\text{III}}$ ($\lambda_{\text{max}} = 695\text{ nm}$, $\epsilon_{\text{max}} = 3.51 \times 10^4\text{ M}^{-1}\text{ cm}^{-1}$) to the $\text{Mn}^{\text{V}}(\text{O})$ complex [$(\text{TBP}_8\text{Cz})\text{Mn}^{\text{V}}(\text{O})$] ($\lambda_{\text{max}} = 634\text{ nm}$, $\epsilon_{\text{max}} = 2.0 \times 10^4\text{ M}^{-1}\text{ cm}^{-1}$)²⁸ with isosbestic points as shown in Figure 1. No further reaction of $(\text{TBP}_8\text{Cz})\text{Mn}^{\text{V}}(\text{O})$ with toluene occurred for another 1 hour (Figure S1 in Supporting Information (SI)), as expected from previous work.^{28,36} No formation of $(\text{TBP}_8\text{Cz})\text{Mn}^{\text{V}}(\text{O})$ was observed in the absence of O_2 or toluene derivatives, indicating both toluene derivatives and O_2 are certainly required to generate $(\text{TBP}_8\text{Cz})\text{Mn}^{\text{V}}(\text{O})$ (Figure S2 and S3 in SI).

The photochemical oxidation of $(\text{TBP}_8\text{Cz})\text{Mn}^{\text{III}}$ with O_2 and hexamethylbenzene to produce $(\text{TBP}_8\text{Cz})\text{Mn}^{\text{V}}(\text{O})$ is accompanied by the oxidation of hexamethylbenzene. Analysis of the reaction mixture by GC-MS reveals the major product of oxidation to be the pentamethylbenzyl alcohol in 87% yield (based on total Mn content), along with a small amount of pentamethylbenzaldehyde (8%) (see Figures S4 – S5, and Table S1 in SI). Thus the oxidation of hexamethylbenzene occurs with high selectivity, and the stoichiometry of the main reaction is given by eqn (6).



Kinetics

Rates of formation of $(\text{TBP}_8\text{Cz})\text{Mn}^{\text{V}}(\text{O})$ in the photochemical oxidation of $(\text{TBP}_8\text{Cz})\text{Mn}^{\text{III}}$ with O_2 in the air and toluene derivatives were determined from the decay of absorbance at 695 nm due to $(\text{TBP}_8\text{Cz})\text{Mn}^{\text{III}}$ in aerated PhCN at 298 K. The zeroth-order rate constant (k_{obs}) was determined from the initial rate in Figure 1b in order to avoid the decrease in the light intensity absorbed by $(\text{TBP}_8\text{Cz})\text{Mn}^{\text{III}}$ in the course of the photochemical reaction. The k_{obs} values were derived from the initial slopes of the plots of $[(\text{TBP}_8\text{Cz})\text{Mn}^{\text{III}}]$ vs time for the different substrates, as shown in Figures S6 – S11 (see Supporting Information). The observed rate constants are proportional to concentrations of substrates, as shown in Figure 2 (see Supporting Information for separate Figures in Figure S12). The rates are also proportional to concentration of O_2 (Figure 3). Thus, the rate law is given by eqn (7), where k_{ox} is a second-order

$$-d[(\text{TBP}_8\text{Cz})\text{Mn}^{\text{III}}]/dt = k_{\text{ox}}[\text{S}][\text{O}_2] \quad (7)$$

Supporting Information for separate Figures in Figure S12). The rates are also proportional to concentration of O_2 (Figure 3). Thus, the rate law is given by eqn (7), where k_{ox} is a second-order rate constant and $[\text{S}]$ is substrates concentration. The slope of the best-fit lines for the k_{obs} values for the different substrates in Figure 2 yield first-order rate constants with respect to substrate concentration. These values can then be divided by the excess O_2 concentration ($1.7 \times 10^{-3} \text{ M}$) to give the second-order rate constants (k_{ox}) listed in Table 1. Interestingly, the second-order rate constants increase with an increasing number of methyl groups in the substrate. A dramatic 200- fold rate enhancement is observed in the presence of hexamethylbenzene over toluene.

When toluene (2.0 M) was replaced with its deuterated analog ($\text{C}_6\text{D}_5\text{CD}_3$), the reaction rate of formation of $(\text{TBP}_8\text{Cz})\text{Mn}^{\text{V}}(\text{O})$ with O_2 became significantly slower as shown in Figure 4a (blue for $\text{C}_6\text{H}_5\text{CH}_3$ and red for $\text{C}_6\text{D}_5\text{CD}_3$). The deuterium kinetic isotope effect (KIE) for toluene was determined to be 5.4. A similar KIE was obtained for the case of mesitylene (KIE = 5.3) as shown in Figure 4b (blue for mesitylene and red for mesitylene- d_{12}). The bond-dissociation energy of the aryl C-H for benzene ($109.8 \text{ kcal mol}^{-1}$) is over 20 kcal mol^{-1} higher than the methyl C-H for toluene ($87.2 \text{ kcal mol}^{-1}$).³⁸ Thus H-atom abstraction from the methyl C-H is dramatically favored, and it is reasonable to expect that H-atom transfer from the methyl C-H occurs rather than from the aryl C-H. In fact, the photochemical reaction of benzene showed negligible formation of $(\text{TBP}_8\text{Cz})\text{Mn}^{\text{V}}(\text{O})$ (Figure S13 in SI). The fact that the methyl group of hexamethylbenzene was oxygenated to yield pentamethylbenzyl alcohol provides additional evidence for this mechanism. Thus the KIE value corresponds to that of H-atom transfer from the methyl C-H rather than the aryl C-H. Taken together, the findings of increasing reaction rate with increasing the number of abstractable hydrogen atoms along with the observed large KIEs suggest that hydrogen-atom

abstraction from the toluene derivative is directly involved in the rate-determining step for the photochemical oxidation of $(\text{TBP}_8\text{Cz})\text{Mn}^{\text{III}}$ with O_2 and toluene derivatives.

Femtosecond Transient Absorption Measurements

In order to detect the photoexcited state involved in the photochemical oxidation of $(\text{TBP}_8\text{Cz})\text{Mn}^{\text{III}}$ with O_2 , the femtosecond laser flash photolysis measurements of $(\text{TBP}_8\text{Cz})\text{Mn}^{\text{III}}$ were performed in the absence and presence of O_2 in PhCN. The Mn^{III} metal ion has a high spin d^4 ground state electronic configuration ($S = 2$) with only the high energy $d_{x^2-y^2}$ orbital unoccupied in the ground state.³⁹ Because of the coupling between unpaired electrons of the metal with the π electrons of the corrolazine ring, the ground state of $(\text{TBP}_8\text{Cz})\text{Mn}^{\text{III}}$ is a singlet ($^5\text{S}_0$). Upon femtosecond laser excitation, instantaneously formed minima at $\lambda_{\text{min}} = 450$ and 695 nm can be observed as shown in Figure 5a which closely mirror the ground-state absorption spectrum (Figure 1a). A new absorption maximum at $\lambda_{\text{max}} = 530$ nm is also formed and can be assigned to the triplet ($^5\text{T}_1$) excited state. It is known that first row paramagnetic complexes, such as Mn^{III} complexes, undergo an extremely rapid intersystem crossing process from the singlet ($^5\text{S}_1$) excited state to the triplet ($^5\text{T}_1$) excited state due to the presence of unpaired electrons.⁴⁰ In Mn^{III} porphyrins, for example, the existence of two tripmultiplet levels was suggested where a triplet ($^5\text{T}_1$) relaxes to a long-lived tripseptet ($^7\text{T}_1$), which requires a spin conversion to go back to the quintet ground state.^{40,41} In the Mn corrolazine complex, we attribute the decay of the absorbance band at 530 nm to intersystem crossing from the $^5\text{T}_1$ state to the $^7\text{T}_1$ state, which has a small absorption band at 774 nm. The decay rate of the triplet ($^5\text{T}_1$) obeyed first-order kinetics with a rate constant of $1.8 \times 10^{10} \text{ s}^{-1}$ in deaerated PhCN (Figure 5b). The similar decay rate constant was observed in O_2 -saturated PhCN (Figure 5c) showing no oxygen dependence on the rate of intersystem crossing.

The absorbance at 774 nm due to $^7\text{T}_1$ remained unchanged up to 3000 ps in deaerated PhCN (Figure 6b), whereas the absorbance decays in O_2 -saturated PhCN (Figure 6c), signaling a direct reaction between the excited state and O_2 . The second-order rate constant of the decay of $[(\text{TBP}_8\text{Cz})\text{Mn}^{\text{III}}]^* (^7\text{T}_1)$ in the presence of O_2 was determined to be $4.9 \times 10^9 \text{ M}^{-1} \text{ s}^{-1}$, which is comparable to the diffusion-limited rate constant in PhCN.⁴² Because the one-electron oxidation potential of $[(\text{TBP}_8\text{Cz})\text{Mn}^{\text{III}}]^* (^7\text{T}_1)$ (-0.90 V vs SCE)⁴³⁻⁴⁵ is more negative than the one-electron reduction potential of O_2 (-0.87 V vs SCE),⁴⁶ electron transfer from $[(\text{TBP}_8\text{Cz})\text{Mn}^{\text{III}}]^* (^7\text{T}_1)$ to O_2 may occur efficiently to produce the Mn(IV)-superoxo complex, $(\text{TBP}_8\text{Cz})\text{Mn}^{\text{IV}}(\text{O}_2^{\bullet-})$.⁴⁷

An alternative mechanism could involve direct energy transfer from $[(\text{TBP}_8\text{Cz})\text{Mn}^{\text{III}}]^* (^7\text{T}_1)$ to O_2 to produce singlet oxygen ($^1\text{O}_2^*$) and the ground state $(\text{TBP}_8\text{Cz})\text{Mn}^{\text{III}}$ ($S = 2$), which is a spin-allowed process. In the initial report on the photochemical oxidation of $(\text{TBP}_8\text{Cz})\text{Mn}^{\text{III}}$ to $(\text{TBP}_8\text{Cz})\text{Mn}^{\text{V}}(\text{O})$, a significant role for singlet oxygen was ruled out by use of the $^1\text{O}_2^*$ trap, 9,10-dimethylanthracene.²⁸ However, to eliminate the possibility of $^1\text{O}_2^*$ as the major oxidant under inert solvent conditions as employed in the present study, we looked for the presence of $^1\text{O}_2^*$ by its phosphorescence spectrum ($\lambda_{\text{max}} = 1270$ nm).^{37,48} The photoexcitation of $(\text{TBP}_8\text{Cz})\text{Mn}^{\text{III}}$ in O_2 -saturated C_6D_6 (PhCN could not be used because of the short lifetime of $^1\text{O}_2$) results in a much smaller phosphorescence signal at 1270 nm than that obtained by photoexcitation of C_{60} under the same conditions.⁴⁹ (see Figure S12 in SI) Thus, the contribution of $^1\text{O}_2^*$ for the photochemical oxidation of $(\text{TBP}_8\text{Cz})\text{Mn}^{\text{III}}$ with O_2 may be negligible as compared with an electron-transfer pathway from $[(\text{TBP}_8\text{Cz})\text{Mn}^{\text{III}}]^* (^7\text{T}_1)$ to O_2 .

Reaction Mechanism

Based on the photodynamics of $(\text{TBP}_8\text{Cz})\text{Mn}^{\text{III}}$, together with the effect of added substrate and the large observed KIEs, the mechanism of photochemical oxidation of $(\text{TBP}_8\text{Cz})\text{Mn}^{\text{III}}$ with O_2 and toluene as the substrate to produce $(\text{TBP}_8\text{Cz})\text{Mn}^{\text{V}}(\text{O})$ is proposed as shown in Scheme 2. Upon photoexcitation of $(\text{TBP}_8\text{Cz})\text{Mn}^{\text{III}}$, the produced triplet excited state ($[(\text{TBP}_8\text{Cz})\text{Mn}^{\text{III}}]^*$ ($^3\text{T}_1$)) is converted rapidly by intersystem crossing to the triplet excited state ($[(\text{TBP}_8\text{Cz})\text{Mn}^{\text{III}}]^*$ ($^7\text{T}_1$)). Electron transfer from $[(\text{TBP}_8\text{Cz})\text{Mn}^{\text{III}}]^*$ ($^7\text{T}_1$) to O_2 occurs to produce the superoxo complex $[(\text{TBP}_8\text{Cz})\text{Mn}^{\text{IV}}(\text{O}_2^{\bullet-})]$. Hydrogen-atom transfer from toluene to $(\text{TBP}_8\text{Cz})\text{Mn}^{\text{IV}}(\text{O}_2^{\bullet-})$ then follows as the rate-determining step, generating the hydroperoxo complex $(\text{TBP}_8\text{Cz})\text{Mn}^{\text{IV}}(\text{OOH})$ and benzyl radical. This reaction is most likely in competition with the back-reaction of electron transfer to regenerate the ground state $(\text{TBP}_8\text{Cz})\text{Mn}^{\text{III}}$ and O_2 . The subsequent homolytic O–O bond cleavage by benzyl radical may occur rapidly inside the reaction cage before the reaction of benzyl radical with O_2 to yield $(\text{TBP}_8\text{Cz})\text{Mn}^{\text{V}}(\text{O})$ and benzyl alcohol (an oxygen rebound pathway). Alternatively, electron transfer may occur from benzyl radical derivatives to $(\text{TBP}_8\text{Cz})\text{Mn}^{\text{IV}}(\text{OOH})$ to produce an ion pair $\{(\text{TBP}_8\text{Cz})\text{Mn}^{\text{III}}(\text{OOH})\}^-$ and benzyl cation $(\text{PhCH}_2)^+$, followed by heterolytic O–O bond cleavage to yield $(\text{TBP}_8\text{Cz})\text{Mn}^{\text{V}}(\text{O})$ and benzyl alcohol derivatives. At present the homolysis vs heterolysis pathway has yet to be distinguished.

According to Scheme 2, the quantum yield of formation of $(\text{TBP}_8\text{Cz})\text{Mn}^{\text{V}}(\text{O})$ is given by eqn (8), where Φ_0 is the quantum yield of photoinduced formation of $(\text{TBP}_8\text{Cz})\text{Mn}^{\text{IV}}(\text{O}_2^{\bullet-})$, k_{H} is the

$$\Phi = \Phi_0 (k_{\text{H}} k_{\text{et}} / (k_{\text{H}} + k_{-\text{et}})) [\text{S}] [\text{O}_2] \quad (8)$$

rate of hydrogen-atom transfer from toluene derivatives (S) to $(\text{TBP}_8\text{Cz})\text{Mn}^{\text{IV}}(\text{O}_2^{\bullet-})$, k_{et} is the rate constant of electron transfer from $[(\text{TBP}_8\text{Cz})\text{Mn}^{\text{III}}]^*$ ($^7\text{T}_1$) to O_2 to produce $(\text{TBP}_8\text{Cz})\text{Mn}^{\text{IV}}(\text{O}_2^{\bullet-})$, and $k_{-\text{et}}$ is the back electron transfer from the $\text{O}_2^{\bullet-}$ moiety to the $(\text{TBP}_8\text{Cz})\text{Mn}^{\text{IV}}$ moiety to regenerate $(\text{TBP}_8\text{Cz})\text{Mn}^{\text{III}}$ and O_2 . Eqn (8) agrees with the empirical rate law [eqn (7)], in which $k_{\text{ox}} = \Phi_0(k_{\text{H}}k_{\text{et}}/(k_{\text{H}} + k_{-\text{et}}))I_n$ (I_n = light intensity absorbed by $(\text{TBP}_8\text{Cz})\text{Mn}^{\text{III}}$).⁵⁰ Because significant KIEs were observed, as shown in Figure 4, the k_{H} value may be much smaller than the $k_{-\text{et}}$ value: $k_{\text{H}} \ll k_{-\text{et}}$, suggesting the back electron transfer pathway is much more favored.

The mechanism in Scheme 2 is similar to O_2 activation by $[(\text{TMC})\text{Fe}^{\text{II}}]^{2+}$ (TMC = 1,4,8,11-tetramethyl-1,4,8,11-tetraazacyclotetradecane) with a hydrogen donor (RH) to produce $[(\text{TMC})\text{Fe}^{\text{IV}}(\text{O})]^{2+}$. In this case, electron transfer from $[(\text{TMC})\text{Fe}^{\text{II}}]^{2+}$ to O_2 occurs thermally to produce $[(\text{TMC})\text{Fe}^{\text{III}}(\text{O}_2^{\bullet-})]^{2+}$. This is followed by hydrogen transfer from RH to $[(\text{TMC})\text{Fe}^{\text{III}}(\text{O}_2^{\bullet-})]^{2+}$ to give R^{\bullet} and $[(\text{TMC})\text{Fe}^{\text{III}}(\text{OOH})]^{2+}$, which undergoes an oxygen rebound reaction via the homolytic O–O bond cleavage by R^{\bullet} to yield $[(\text{TMC})\text{Fe}^{\text{IV}}(\text{O})]^{2+}$ and ROH.⁵¹

If a free radical (e.g., pentamethylbenzyl radical) were produced following hydrogen-atom transfer from a toluene derivative to $(\text{TBP}_8\text{Cz})\text{Mn}^{\text{IV}}(\text{O}_2^{\bullet-})$, the benzyl radical should react with O_2 to produce the peroxy radical, which may act as a chain carrier for the autoxidation of hexamethylbenzene to produce pentamethylbenzyl hydroperoxide. The disproportionation of the peroxy radical may yield equimolar pentamethylbenzyl alcohol and pentamethylbenzaldehyde. The fact that neither pentamethylbenzyl hydroperoxide nor pentamethylbenzaldehyde were produced and that pentamethylbenzyl alcohol was the major product, provides strong evidence for the conclusion that the rebound pathway to produce pentamethylbenzyl alcohol is faster than the rate of the reaction of pentamethylbenzyl radical with O_2 . Judging from the reported rate constant of benzyl radical with O_2 (2.6×10^9

$M^{-1} s^{-1}$)⁵² to produce benzyl peroxy radical, and the O_2 concentration (8.5 mM) of the reaction mixture, the lifetime of the radical is expected to be shorter than 45 ns = $(2.6 \times 10^9 \times 8.5 \times 10^{-3})^{-1}$. The lifetime of $(TBP_8Cz)Mn^{IV}(OOH)$ is also expected to be shorter than 45 ns. In such a case, it is very difficult to detect $(TBP_8Cz)Mn^{IV}(OOH)$, because this is a high energy species, which goes back to $(TBP_8Cz)Mn^{III}$, O_2 and H^+ .^{53,54}

Comparison of Hydrogen Transfer Reactivity

In order to gain deeper insight into the rate-determining hydrogen transfer from toluene derivatives to $(TBP_8Cz)Mn^{IV}(O_2^{\bullet-})$, the reactivity was compared with that of hydrogen transfer from the same toluene derivatives employed in this study to cumylperoxy radical, which is regarded as an authentic hydrogen-transfer reaction.^{35,55,56} The rates of hydrogen transfer from toluene derivatives to cumylperoxy radical were determined by monitoring the reactions by EPR spectroscopy. Cumylperoxy radicals were generated by photoirradiation of an aerated propionitrile solution containing di-*tert*-butylperoxide ($tBuOOtBu$) and cumene [$PhCH(CH_3)_2$] with a 1000 W Mercury lamp via a radical chain process as shown in Scheme 3.³⁵ The UV light irradiation of $tBuOOtBu$ results in the O–O bond cleavage to produce $tBuO^{\bullet}$. This radical can then readily abstract a hydrogen from cumene to generate cumyl radical [$PhC^{\bullet}(CH_3)_2$]. Rapid O_2 addition to the cumyl radical affords the cumylperoxy radical ($PhC(CH_3)_2OO^{\bullet}$). Once generated, this autoxidation process continues until cumylperoxy radicals decay via β -scission producing acetophenone and CH_3O^{\bullet} .⁵⁷

After cutting off the light, the decay rates of cumylperoxy radical were monitored by the decrease of EPR signal intensity at $g = 2.0156$ in the presence of a toluene derivative in propionitrile at 193 K, as shown in Figure 7. The decay rates of cumylperoxy radical obeyed first-order kinetics under the conditions with large excess toluene derivatives.⁵⁸ The pseudo-first-order rate constants (k'_{obs}) were linearly proportional to concentrations of toluene derivatives as shown in Figure 8. The second-order rate constants (k'_H) of the hydrogen atom transfer from toluene derivatives to cumylperoxy radicals were determined from the slopes of linear plots in Figure 8. The k'_H values are also listed in Table 1. The decay rates of cumylperoxy radical in the presence of a toluene derivative become faster than in the absence of the toluene derivative.

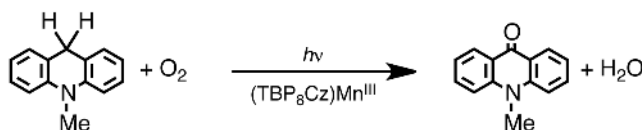
These results suggest that hydrogen-atom transfer from the toluene derivative to cumylperoxy radical readily occurs. Figure 9 shows plots of the logarithm of the k_{ox} values of the photochemical oxidation of $(TBP_8Cz)Mn^{III}$ with O_2 in the presence of toluene derivatives and the k'_H values of hydrogen-atom transfer from toluene derivatives to cumylperoxy radicals vs the one-electron oxidation peak potentials of the toluene derivatives (E^{POX}), which were reported previously.⁵⁹ There is a linear correlation between $\log k_{ox}$ and E^{POX} with a larger slope (3.2) than that between $\log k'_H$ and E^{POX} (1.7) in Figure 9. The slopes of 3.2 and 1.7 correspond to 19% ($3.2/16.9$) and 7% ($2.2/26.0$) of the difference in the free energy change of electron transfer, because the difference in 1 V of E_{ox} corresponds to the difference in terms of logarithm of the rate constant to be $2.3RT = 26.0$ and 16.9 at 193 and 298 K, respectively. The k'_H value of hexamethylbenzene increases by a factor of 20 as compared with that of toluene, while the number of hydrogen atoms increases by a factor of 6. Thus, a small ca. 3-fold “net” increase was observed in the rates of cumylperoxy radical decay rate in the presence of hexamethylbenzene compared to its reaction with toluene. In general, the k'_H value is expected to increase with decreasing the C–H bond dissociation energies of toluene derivatives.⁶⁰ However, the C–H bond dissociation energies of toluene derivatives have been reported to be only slightly affected by the electron-donating or –withdrawing substituents.⁶¹ The small “net” difference in the hydrogen-transfer reactivity of cumylperoxy radical with hexamethylbenzene vs toluene

results from the small change in the C-H bond dissociation energies of toluene derivatives. The larger slope (3.2) in the plot of $\log k_{\text{ox}}$ vs E^{POX} than the slope (1.7) in the plot of $\log k'_{\text{H}}$ and E^{POX} in Figure 9 indicates the higher degree of charge transfer in the transition state of the hydrogen-transfer reactions of $(\text{TBP}_8\text{Cz})\text{Mn}^{\text{IV}}(\text{O}_2^{\bullet-})$ as compared with those of cumylperoxy radical, as reported for the linear relations between logarithm of the rate constants of hydrogen-transfer reactions of triplet excited state of acetophenone derivatives and the ionization potentials of hydrogen donors.⁶²

Photocatalytic Reactivity with AcrH₂

The photocatalytic reactivity of $(\text{TBP}_8\text{Cz})\text{Mn}^{\text{III}}$ was examined under irradiation (white light) of a reaction solution (0.5 mL) containing $(\text{TBP}_8\text{Cz})\text{Mn}^{\text{III}}$ (1.7×10^{-4} M) and AcrH₂ (0.2 M) which has a weaker C-H bond than toluene derivatives. The time course for formation of Acr=O as the product quantified by absorbance at 402 nm ($\lambda = 402$ nm, $\epsilon_{\text{max}} = 8.6 \times 10^3$ M⁻¹ cm⁻¹)⁶³ is shown in Figure 10a. The turnover number was determined to be 11 in 5 hours based on the initial amount of $(\text{TBP}_8\text{Cz})\text{Mn}^{\text{III}}$. A negligible amount of Acr=O was produced from a reaction solution without $(\text{TBP}_8\text{Cz})\text{Mn}^{\text{III}}$ as a control experiment.

When AcrH₂ was replaced by the dideuterated compound AcrD₂, the photocatalytic reactivity dramatically decreased with a large kinetic deuterium isotope (KIE) value of 16 as shown in Figure 10b (blue for AcrH₂ and red for AcrD₂).⁶⁴ This KIE suggests that hydrogen-atom transfer from AcrH₂ to $(\text{TBP}_8\text{Cz})\text{Mn}^{\text{IV}}(\text{O}_2^{\bullet-})$ is involved in the rate-determining step as seen in the case of toluene derivatives in Scheme 2. This hydrogen transfer may also proceed via electron transfer from AcrH₂ to $(\text{TBP}_8\text{Cz})\text{Mn}^{\text{IV}}(\text{O}_2^{\bullet-})$, followed by rate-limiting proton transfer from AcrH₂^{•+} to $(\text{TBP}_8\text{Cz})\text{Mn}^{\text{IV}}(\text{O}_2^{2-})$ to produce AcrH[•] and $(\text{TBP}_8\text{Cz})\text{Mn}^{\text{IV}}(\text{OOH}^-)$. As seen for the toluene derivatives, oxygen rebound via homolytic O–O bond cleavage by AcrH[•] yields $(\text{TBP}_8\text{Cz})\text{Mn}^{\text{V}}(\text{O})$ and AcrHOH. The electron-donating OH group in AcrHOH may make it easier to be oxidized by $(\text{TBP}_8\text{Cz})\text{Mn}^{\text{V}}(\text{O})$ as compared to AcrH₂ via electron and proton transfer, yielding Acr=O and regenerating $(\text{TBP}_8\text{Cz})\text{Mn}^{\text{III}}$ (Scheme 4). The stoichiometry of the photocatalytic reaction is given by eqn (9). The slow catalytic oxidation of AcrH₂ may result from the much faster back electron transfer in $(\text{TBP}_8\text{Cz})\text{Mn}^{\text{IV}}(\text{O}_2^{\bullet-})$ as compared with the hydrogen-transfer reaction with AcrH₂ in Scheme 4.



(9)

CONCLUSIONS

Photoirradiation of $(\text{TBP}_8\text{Cz})\text{Mn}^{\text{III}}$ with O₂ and toluene derivatives in the inert solvent PhCN results in the rare formation of a high-valent manganese(V)-oxo complex with O₂ as the oxidant. At the same time, the substrate hexamethylbenzene is selectively oxidized in good yield to a single, mono-hydroxylated benzyl alcohol product. The photochemical mechanism was interrogated by femtosecond laser flash photolysis measurements, leading to the first direct spectroscopic observation of a novel photo-excited state ($[(\text{TBP}_8\text{Cz})\text{Mn}^{\text{III}}]^*$ (⁷T₁)), which was found to be responsible for the initial reaction with O₂. The LFP experiments, together with kinetic studies involving substrate dependence and KIEs,

indicate that the mechanism of photochemical oxidation involves the short-lived 7T_1 excited state reacting with O_2 via binding and electron-transfer to produce the proposed superoxo complex $(TBP_8Cz)Mn^{IV}(O_2^{\bullet-})$. The superoxo complex then abstracts a hydrogen atom from the toluene derivatives in the rate-determining step to produce $(TBP_8Cz)Mn^{IV}(O_2H)$, followed by oxygen rebound of the resulting benzyl radical derivatives with $(TBP_8Cz)Mn^{IV}(OOH)$ to yield the corresponding benzyl alcohol derivatives and $(TBP_8Cz)Mn^V(O)$ (Scheme 2). The hydrogen-atom abstracting reactivity of cumylperoxy radical was examined with the same set of toluene derivatives, and comparison of the kinetic data confirmed that H-atom abstraction was the rate-determining step for the Mn complex, and indicated that the putative $(TBP_8Cz)Mn^{IV}(O_2^{\bullet-})$ species exhibited more electrophilic character toward H-atom transfer than the cumylperoxy radical. Our mechanistic findings suggested that catalytic oxidations should be possible with the appropriate substrate, and indeed, it was shown that carrying out the reaction with a stronger hydrogen donor such as $AcRH_2$ leads to the photocatalytic oxidation of this substrate by O_2 and $(TBP_8Cz)Mn^{III}$ as catalyst. We have thus revealed a new method for the selective oxidation of benzylic C-H bonds involving only O_2 , light and a discrete Mn^{III} complex. The mechanistic findings and accompanying model (Scheme 2) provide valuable insights into the generation of high-valent metal-oxo intermediates via O_2 activation in the presence of a hydrogen-atom (electron and proton) source.

Supplementary Material

Refer to Web version on PubMed Central for supplementary material.

Acknowledgments

This work was supported by Grants-in-Aid (No. 20108010 to S.F. and 23750014 to K.O.), the NSF (CHE0909587 and CHE121386 to D.P.G.), the NIH (GM101153 to D.P.G) by a Grant-in-Aid (20108010) and a Global COE Program ("The Global Education and Research Center for Bio-Environmental Chemistry") from the Ministry of Education, Culture, Sports, Science, and Technology, Japan, and by KOSEF/MEST through the WCU Project (R31-2008-000-10010-0). K.A.P. is grateful for a Harry and Cleio Greer Fellowship.

REFERENCES

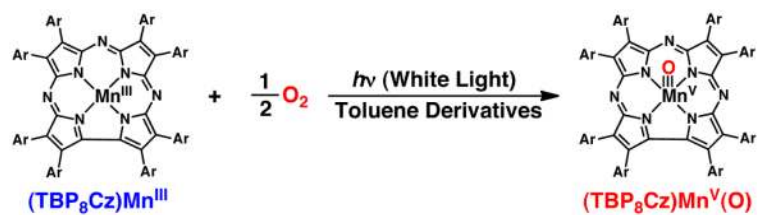
- (a) Ortiz de Montellano, PR., editor. *Cytochrome P450: Structure, Mechanism and Biochemistry*. 3rd. Kluwer; New York: 2004. (b) Rittle J, Green MT. *Science*. 2010; 330:933–937. [PubMed: 21071661] (c) Meunier, B., editor. *Metal-Oxo and Metal-Peroxo Species in Catalytic Oxidations*. Springer-Verlag; Berlin: 2000. (d) Ortiz de Montellano, PR., editor. *Cytochrome P450: Structure, Mechanism, and Biochemistry*. 3rd. Kluwer Academic/Plenum Publishers; New York: 2005.
- (a) Sono M, Roach MP, Coulter ED, Dawson JH. *Chem. Rev.* 1996; 96:2841–2888. [PubMed: 11848843] (b) Groves JT. *Proc. Natl. Acad. Sci. U.S.A.* 2003; 100:3569–3574. [PubMed: 12655056] (c) Denisov IG, Makris TM, Sligar SG, Schlichting I. *Chem. Rev.* 2005; 105:2253–2277. [PubMed: 15941214] (d) Makris TM, von Koenig K, Schlichting I, Sligar SGJ. *Inorg. Biochem.* 2006; 100:507–518. (e) Meunier B, de Visser SP, Shaik S. *Chem. Rev.* 2004; 104:3947–3980. [PubMed: 15352783]
- (a) Betley TA, Wu Q, Voorhis TV, Nocera DG. *Inorg. Chem.* 2008; 47:1849–1861. [PubMed: 18330975] (b) Mullins C, Pecoraro VL. *Coord. Chem. Rev.* 2008; 252:416–443. [PubMed: 19081816] (c) Cady CW, Crabtree RH, Brudvig GW. *Coord. Chem. Rev.* 2008; 252:444–455. [PubMed: 21037800] (d) Wydrzynski, T.; Satoh, K., editors. *Advances in Photosynthesis and Respiration*. Vol. 22. Springer; Dordrecht, The Netherlands: 2005. *Photosystem II: The Light-Driven Water: Plastoquinone Oxidoreductase*.
- (a) McEvoy JP, Brudvig GW. *Chem. Rev.* 2006; 106:4455–4483. [PubMed: 17091926] (b) Betley TA, Wu Q, Van Voorhis T, Nocera DG. *Inorg. Chem.* 2008; 47:1849–1861. [PubMed: 18330975] (c) Umena Y, Kawakami K, Shen JR, Kamiya N. *Nature*. 2011; 473:55–60. [PubMed: 21499260] (d) Barber J. *Inorg. Chem.* 2008; 47:1700–1710. [PubMed: 18330964]

5. (a) Meunier B. *Chem. Rev.* 1992; 92:1411–1456. (b) D., Mansuy. *Coord. Chem. Rev.* 1993; 125:129–142. (c) Groves, JT. *Cytochrome P450: Structure, Mechanism, and Biochemistry*. 3rd. Ortiz de Montellano, PR., editor. Kluwer Academic/Plenum Publishers; New York: 2005. p. 1-43. (d) Groves JT, Lee J, Marla SS. *J. Am. Chem. Soc.* 1997; 119:6269–6273. (e) Jin N, Groves JT. *J. Am. Chem. Soc.* 1999; 121:2923–2924.
6. (a) Nam W. *Acc. Chem. Res.* 2007; 40:465–465. (b) Nam, W. *Comprehensive Coordination Chemistry II: From Biology to Nanotechnology*. Que, L., Jr.; Tolman, WT., editors. Vol. 8. Elsevier Ltd.; Oxford: 2004. p. 281-307.
7. (a) Martinho M, Blain G, Banse F. *Dalton Trans.* 2010; 39:1630–1634. [PubMed: 20104327] (b) Hong S, Lee Y-M, Shin W, Fukuzumi S, Nam W. *J. Am. Chem. Soc.* 2009; 131:13910–13911. [PubMed: 19746912] (c) Thibon A, England J, Martinho M, Young VG Jr, Frisch JR, Guillot R, Girerd J-J, Munck E, Que L Jr, Banse F. *Angew. Chem., Int. Ed.* 2008; 47:7064–7067.
8. (a) Fujii H. *Coord. Chem. Rev.* 2002; 226:51–60. (b) McLain, JL.; Lee, J.; Groves, JT. *Biomimetic Oxidations Catalyzed by Transition Metal Complexes*. Meunier, B., editor. Imperial College Press; London: 2000. p. 91-169. (c) Watanabe, Y. *The Porphyrin Handbook*. Kadish, KM.; Smith, KM.; Guillard, R., editors. Vol. 4. Vol. 30. Academic; New York: 2000. p. 97-117.
9. (a) Sawada Y, Matsumoto K, Katsuki T. *Angew. Chem., Int. Ed.* 2007; 46:4559–4561. (b) Fujita M, Costas M, Que L Jr. *J. Am. Chem. Soc.* 2003; 125:9912–9913. [PubMed: 12914440]
10. (a) Battioni P, Renaud JP, Bartoli JF, Reinaartiles M, Fort M, Mansuy D. *J. Am. Chem. Soc.* 1988; 110:8462–8470. (b) Bernadou J, Fabiano A-S, Robert A, Meunier B. *J. Am. Chem. Soc.* 1994; 116:9375–9376.
11. (a) Jin N, Bourassa JL, Tizio SC, Groves JT. *Angew. Chem., Int. Ed.* 2000; 39:3849–3851. (b) Nam W, Kim I, Lim MH, Choi HJ, Lee JS, Jang HG. *Chem.–Eur. J.* 2002; 8:2067–2071. [PubMed: 11981891] (c) Zhang R, Newcomb M. *J. Am. Chem. Soc.* 2003; 125:12418–12419. [PubMed: 14531679] (d) Zhang R, Horner JH, Newcomb M. *J. Am. Chem. Soc.* 2005; 127:6573–6582. [PubMed: 15869278] (e) Shimazaki Y, Nagano T, Takesue H, Ye B-H, Tani F, Naruta Y. *Angew. Chem., Int. Ed.* 2004; 43:98–100.
12. McLain, JL.; Lee, J.; Groves, JT. *Biomimetic Oxidations Catalyzed by Transition Metal Complexes*. Meunier, B., editor. Imperial College Press; London: 2000. p. 91-169.
13. Gross Z, Golubkov G, Simkhovich L. *Angew. Chem., Int. Ed.* 2000; 39:4045–4047.
14. (a) Nam W, Jin SW, Lim MH, Ryu JY, Kim C. *Inorg. Chem.* 2002; 41:3647–3652. [PubMed: 12099867] (b) Nam W, Kim I, Lim MH, Choi HJ, Lee JS, Jang HG. *Chem.–Eur. J.* 2002; 8:2067–2071. [PubMed: 11981891] (c) Fukuzumi S, Kishi T, Kotani H, Lee Y-M, Nam W. *Nat. Chem.* 2011; 3:38–41. [PubMed: 21160515]
15. (a) Reginato G, Di Bari L, Salvadori P, Guillard R. *Eur. J. Org. Chem.* 2000:1165–1171. (b) Battioni P, Cardin E, Louloudi M, Schollhorn B, Spyroulias GA, Mansuy D, Traylor TG. *Chem. Commun.* 1996:2037–2038. (c) Nishiyama H, Shimada T, Itoh H, Sugiyama H, Motoyama Y. *Chem. Commun.* 1997:1863–1864.
16. Liu HY, Lai TS, Yeung LL, Chang CK. *Org. Lett.* 2003; 5:617–620. [PubMed: 12605473]
17. (a) Low DW, Winkler JR, Gray HB. *J. Am. Chem. Soc.* 1996; 118:117–120. (b) Berglund J, Pascher T, Winkler JR, Gray HB. *J. Am. Chem. Soc.* 1997; 119:2464–2469.
18. (a) Hirai Y, Kojima T, Mizutani Y, Shiota Y, Yoshizawa K, Fukuzumi S. *Angew. Chem., Int. Ed.* 2008; 47:5772–5776. (b) Kojima T, Hirai Y, Ikemura K, Ogura T, Shiota Y, Yoshizawa K, Fukuzumi S. *Angew. Chem., Int. Ed.* 2010; 49:8449–8453. (c) Sawant SC, Wu X, Cho J, Cho K-B, Kim SH, Seo MS, Lee Y-M, Kubo M, Ogura T, Shaik S, Nam W. *Angew. Chem., Int. Ed.* 2010; 49:8190–8194. (d) Kojima T, Nakayama K, Ikemura K, Ogura T, Fukuzumi S. *J. Am. Chem. Soc.* 2011; 133:11692–11700. [PubMed: 21696162]
19. (a) Bozoglian F, Romain S, Erten MZ, Todorova TK, Sens C, Mola J, Rodóriguez M, Romero I, Benet-Buchholz J, Fontrodona X, Cramer CJ, Gagliardi L, Llobet A. *J. Am. Chem. Soc.* 2009; 131:15176–15187. [PubMed: 19791789] (b) Sartorel A, Miró P, Salvadori E, Romain S, Carrano M, Scorrano G, Valentin MD, Llobet A, Bonchio M. *J. Am. Chem. Soc.* 2009; 131:16051–16053. [PubMed: 19842627]
20. (a) Kotani H, Suenobu T, Lee Y-M, Nam W, Fukuzumi S. *J. Am. Chem. Soc.* 2011; 133:3249–3251. [PubMed: 21329389] (b) Kalita D, Radaram B, Brooks B, Kannam PP, Zhao X.

- ChemCatChem. 2011; 3:571–573.(c) Li F, Yu M, Jiang Y, Huang F, Li Y, Zhang B, Sun L. Chem. Commun. 2011; 47:8949–8951.
21. Sartorel A, Carraro M, Scorrano G, Zorzi RD, Geremia S, McDaniel ND, Bernhard S, Bonchio M. J. Am. Chem. Soc. 2008; 130:5006–5007. [PubMed: 18345628]
 22. (a) Geletii YV, Huang Z, Hou Y, Musaev DG, Lian T, Hill CL. J. Am. Chem. Soc. 2009; 131:7522–7523. [PubMed: 19489637] (b) Besson C, Huang Z, Geletii YV, Lense S, Hardcastle KI, Musaev DG, Lian T, Proust A, Hill CL. Chem. Commun. 2010; 46:2784–2786.
 23. (a) Moyer BA, Thompson MS, Meyer TJ. J. Am. Chem. Soc. 1980; 102:2310–2312.(b) Moyer BA, Meyer TJ. Inorg. Chem. 1981; 20:436–444.(c) Che C-M, Yam VW-W, Mak TCW. J. Am. Chem. Soc. 1990; 112:2284–2291.(d) Szczepura LF, Maricich SM, See RF, Churchill MR, Takeuchi KJ. Inorg. Chem. 1995; 34:4198–4205.(e) Che C-M, Cheng K-W, Chan MCW, Lau T-C, Mak C-K. J. Org. Chem. 2000; 65:7996–8000. [PubMed: 11073609] (f) Meyer TJ, Huynh MHV. Inorg. Chem. 2003; 42:8140–8160. [PubMed: 14658865] (g) Dhuri SN, Seo MS, Lee Y-M, Hirao H, Wang Y, Nam W, Shaik S. Angew. Chem., Int. Ed. 2008; 47:3356–3359.
 24. (a) Tabushi I. Coord. Chem. Rev. 1988; 86:1–42.(b) Fukuzumi S, Mochizuki S, Tanaka T. Isr. J. Chem. 1988; 28:29–36.
 25. (a) Hong S, Lee Y-M, Shin W, Fukuzumi S, Nam W. J. Am. Chem. Soc. 2009; 131:13910–13911. [PubMed: 19746912] (b) Lee Y-M, Hong S, Morimoto Y, Shin W, Fukuzumi S, Nam W. J. Am. Chem. Soc. 2010; 132:10668–10670. [PubMed: 20681694]
 26. (a) O'Reilly ME, Del Castillo TJ, Falkowski JM, Ramachandran V, Pati M, Correia MC, Abboud KA, Dalal NS, Richardson DE, Veige AS. J. Am. Chem. Soc. 2011; 133:13661–13673. [PubMed: 21780813] (b) Egorova OA, Tsay OG, Khatua S, Huh JO, Churchill DG. Inorg. Chem. 2009; 48:4634–4636. [PubMed: 19371066]
 27. (a) Meier-Callahan AE, Gray HB, Gross Z. Inorg. Chem. 2000; 39:3605–3607. [PubMed: 11196822] (b) Meier-Callahan AE, Di Bilio AJ, Simkhovich L, Mahammed A, Goldberg I, Gray HB, Gross Z. Inorg. Chem. 2001; 40:6788–6793. [PubMed: 11735492] (c) Mahammed A, Gray HB, Meier-Callahan AE, Gross Z. J. Am. Chem. Soc. 2003; 125:1162–1163. [PubMed: 12553806] (d) Egorova OA, Tsay OG, Khatua S, Meka B, Maiti N, Kim MK, Kwon SJ, Huh JO, Bucella D, Kang SO, Kwak J, Churchill DG. Inorg. Chem. 2010; 49:502–512. [PubMed: 20017519]
 28. Prokop KA, Goldberg DP. J. Am. Chem. Soc. 2012; 134:8014–8017. [PubMed: 22533822]
 29. (a) Rosenthal J, Luckett TD, Hodgkiss JM, Nocera DG. J. Am. Chem. Soc. 2006; 128:6546–6547. [PubMed: 16704240] (b) Pistorio BJ, Chang CJ, Nocera DG. J. Am. Chem. Soc. 2002; 124:7884–7885. [PubMed: 12095316] (c) Harischandra DN, Lowery G, Zhang R, Newcomb M. Org. Lett. 2009; 11:2089–2092. [PubMed: 19361171] (d) Vanover E, Huang Y, Xu LB, Newcomb M, Zhang R. Org. Lett. 2010; 12:2246–2249. [PubMed: 20394434] (e) Peterson MW, Rivers DS, Richman RM. J. Am. Chem. Soc. 1985; 107:2907–2915.(f) Ghosh A, de Oliveira FT, Yano T, Nishioka T, Beach ES, Kinoshita I, Münck E, Ryabov AD, Horwitz CP, Collins TJ. J. Am. Chem. Soc. 2005; 127:2505–2513. For a closely related nonporphyrin Fe–O–Fe complex. [PubMed: 15725005]
 30. (a) Suslick KS, Watson RA. New J. Chem. 1992; 16:633–642.(b) Maldotti A, Amadelli R, Bartocci C, Carassiti V, Polo E, Varani G. Coord. Chem. Rev. 1993; 125:143–154.(c) Maldotti A, Bartocci C, Varani G, Molinari A, Battioni P, Mansuy D. Inorg. Chem. 1996; 35:1126–1131. [PubMed: 11666299] (d) Maldotti A, Andreotti L, Molinari A, Carassiti V. J. Biol. Inorg. Chem. 1999; 4:154–161. [PubMed: 10499085]
 31. (a) Lansky DE, Mandimutsira B, Ramdhanie B, Clausen M, Penner-Hahn J, Zvyagin SA, Telser J, Krzystek J, Zhan R, Ou Z, Kadish KM, Zakharov L, Rheingold AL, Goldberg DP. Inorg. Chem. 2005; 44:4485–4498. [PubMed: 15962955] (b) Ramdhanie B, Stern CL, Goldberg DP. J. Am. Chem. Soc. 2001; 123:9447–9448. [PubMed: 11562230] (c) Mandimutsira BS, Ramdhanie B, Todd RC, Wang HL, Zareba AA, Czernuszewicz RS, Goldberg DP. J. Am. Chem. Soc. 2002; 124:15170–15171. [PubMed: 12487581]
 32. Armarego, WLF.; Perrin, DD., editors. Purification of Laboratory Chemicals. Pergamon Press; Oxford: 1997.
 33. Fukuzumi S, Ohkubo K, Tokuda Y, Suenobu T. J. Am. Chem. Soc. 2000; 122:4286–4294.
 34. Hatchard CG, Parker CA. Proc. R. Soc. London, Ser. A. 1956; 235:518–536.
 35. (a) Fukuzumi S, Shimoosako K, Suenobu T, Watanabe Y. J. Am. Chem. Soc. 2003; 125:9074–9082. [PubMed: 15369364] (b) Matsumoto T, Ohkubo K, Honda K, Yazawa A, Furutachi H,

- Fujinami S, Fukuzumi S, Suzuki M. *J. Am. Chem. Soc.* 2009; 131:9258–9267. [PubMed: 19530656] (c) Osako T, Ohkubo K, Taki M, Tachi Y, Fukuzumi S, Itoh S. *J. Am. Chem. Soc.* 2003; 125:11027–11033. [PubMed: 12952484] (d) Ohkubo K, Moro-oka Y, Fukuzumi S. *Org. Biomol. Chem.* 2006; 4:999–1001. [PubMed: 16525542] (e) Nakanishi I, Miyazaki K, Shimada T, Ohkubo K, Urano S, Ikota N, Ozawa T, Fukuzumi S, Fukuhara K. *J. Phys. Chem. A.* 2002; 106:11123–11126. (f) Nakanishi I, Uto Y, Ohkubo K, Ozawa T, Fukuhara K, Fukuzumi S, Nagasawa H, Hori H, Ikota N. *Org. Biomol. Chem.* 2003; 1:1452–1454. [PubMed: 12926271]
36. (a) Lansky DE, Goldberg DP. *Inorg. Chem.* 2006; 45:5119–5125. [PubMed: 16780334] (b) Prokop KA, Visser SP, Goldberg, D. P. *Angew. Chem., Int. Ed.* 2010; 49:5091–5095.
37. Fukuzumi S, Ohkubo K, Chen Y, Pandey RK, Zhan R, Shao J, Kadish KM. *J. Phys. Chem. A.* 2002; 106:5105–5113.
38. Berkowitz J, Ellison CB, Gutman D. *J. Phys. Chem.* 1994; 98:2744–2765.
39. (a) Rodriguez J, Holten D. *J. Chem. Phys.* 1989; 91:3525–3531. (b) Humphrey JL, Kuciauskas D. *J. Am. Chem. Soc.* 2006; 128:3902–3903. [PubMed: 16551085]
40. (a) Yan X, Kirmaier C, Holten D. *Inorg. Chem.* 1986; 25:4774–4777. (b) Gonçalves P, De Boni L.; Borissevitch IE, Zilio SC. *J. Phys. Chem. A.* 2008; 112:6522–6526. [PubMed: 18588273]
41. Krokos E, Spänig F, Ruppert M, Hirsch A, Guldi DM. *Chem.–Eur. J.* 2012; 18:1328–1341. [PubMed: 22213484]
42. (a) Fukuzumi S, Suenobu T, Patz M, Hirasaka T, Itoh S, Fujitsuka M, Ito O. *J. Am. Chem. Soc.* 1998; 120:8060–8068. (b) Kawashima Y, Ohkubo K, Fukuzumi S. *J. Phys. Chem. A.* 2013; 117:6737–6743. [PubMed: 23862971]
43. The one-electron oxidation potential of [(TBP₈Cz)Mn^{III}]^{*} (⁷T₁) is estimated by subtracting the ⁷T₁ excited state energy (1.59 eV)⁴⁴ from the one-electron oxidation potential of the ground state.⁴⁵
44. Brookfieldh RL, Llula E, Harriman. The ⁷T₁ excited state energy was taken from the value of Mn^{III}TPP. *J. Chem. Soc., Faraday Trans. 2.* 1985; 81:1837–1848.
45. Fukuzumi S, Kotani H, Prokop KA, Goldberg DP. *J. Am. Chem. Soc.* 2011; 133:1859–1869. [PubMed: 21218824]
46. (a) Sawyer DT, Chiericato G Jr, Angelis CT, Nanni EJ Jr, Tsuchiya T. *Anal. Chem.* 1982; 54:1720–1724. (b) Kawashima T, Ohkubo K, Fukuzumi S. *Phys. Chem. Chem. Phys.* 2011; 13:3344–3352. [PubMed: 21212887] (c) Fukuzumi S, Fujita S, Suenobu T, Yamada H, Imahori H, Araki Y, Ito O. *J. Phys. Chem. A.* 2002; 106:1241–1247.
47. The binding of O₂^{•-} to [(TBP₈Cz)Mn^{IV}]⁺ may facilitate the electron-transfer reaction, because the electron-transfer product is more stabilized thermodynamically..
48. (a) Fukuzumi S, Ohkubo K, Zheng X, Chen Y, Pandey RK, Zhan R, Kadish KM. *J. Phys. Chem. B.* 2008; 112:2738–2746. [PubMed: 18254618] (b) Tanaka M, Ohkubo K, Fukuzumi S. *J. Phys. Chem. A.* 2006; 110:11214–11218. [PubMed: 16986858]
49. (a) Araki Y, Dobrowolski DC, Goyne TE, Hanson DC, Jiang ZQ, Lee KJ, Foote CS. *J. Am. Chem. Soc.* 1984; 106:4570–4575. (b) Fukuzumi S, Fujita S, Suenobu T, Yamada H, Imahori H, Araki Y, Ito O. *J. Phys. Chem. A.* 2002; 106:1241–1247.
50. The maximum quantum yield for the formation of (TBP₈Cz)Mn^V(O) was determined to be 0.028% for hexamethylbenzene (0.10 M)..
51. Kim SO, Sastri CV, Seo MS, Kim J, Nam W. *J. Am. Chem. Soc.* 2005; 127:4178–4179. [PubMed: 15783193]
52. Tokumura K, Ozaki T, Nosaka H, Saigusa Y, Itoh M. *J. Am. Chem. Soc.* 1991; 113:4974–4980.
53. A radical clock substrate (*trans*-1-methyl-2-phenylcyclopropane) with fast rearrangement ($4 \times 10^{11} \text{ s}^{-1}$)⁵⁴ may be useful to confirm the oxygen rebound mechanism in Scheme 2. Appropriate radical clocks which have enough reactivity with (TBP₈Cz)Mn^{IV} (O₂^{•-}) should be chosen to gain more insights into the lifetimes of substrate radicals in the rebound pathway for the future study..
54. Atkinson JK, Hollenberg PF, Ingold KU, Johnson CC, Le Tadic M-H, Newcomb M, Putt DA. *Biochemistry.* 1994; 33:10630–10637. [PubMed: 8075063]
55. (a) Parshall, GW.; Ittel, SD. *Homogeneous Catalysis.* 2nd. Wiley; New York: 1992. Chap. 10(b) Sheldon RA, Kochi JK. *Adv. Catal.* 1976; 25:272–413.

56. (a) Kochi JK, Krusic PJ, Eaton DR. *J. Am. Chem. Soc.* 1969; 91:1877–1879.(b) Krusic PJ, Kochi JK. *J. Am. Chem. Soc.* 1968; 90:7155–7157.(c) Krusic PJ, Kochi JK. *J. Am. Chem. Soc.* 1969; 91:3938–3940.(d) Krusic PJ, Kochi JK. *J. Am. Chem. Soc.* 1969; 91:3942–3944.(e) Kochi JK, Krusic PJ. *J. Am. Chem. Soc.* 1969; 91:3944–3946.(f) Howard JA, Furimsky E. *Can. J. Chem.* 1974; 52:555–556.
57. (a) Fukuzumi S, Ono Y. *J. Chem. Soc., Perkin Trans. 2.* 1977:622–625.(b) Fukuzumi S, Ono Y. *J. Chem. Soc., Perkin Trans. 2.* 1977:625–630.(c) Hendry DG. *J. Am. Chem. Soc.* 1967; 89:5433–5438.(d) Zwolenik JJ. *J. Phys. Chem.* 1967; 71:2464–2469.(e) Bennett JE, Brown DM, Mile B. *Trans. Faraday Soc.* 1970; 68:397–405.
58. The concentration of cumylperoxyl radical generated in an EPR tube under photoirradiation is $\sim 10^{-6}$ M calculated by the integration of EPR spectrum..
59. (a) Fukuzumi S, Ohkubo K, Suenobu T, Kato K, Fujitsuka M, Ito OJ. *Am. Chem. Soc.* 2001; 123:8459–8467.(b) Murakami M, Ohkubo K, Fukuzumi S. *Chem.–Eur. J.* 2010; 16:7820–7832. [PubMed: 20496351]
60. Mayer JM. *Acc. Chem. Res.* 1998; 31:441–450.
61. Wu Y-D, Wong C-L, Chan KWK. *J. Org. Chem.* 1996; 61:746–750. [PubMed: 11666999]
62. (a) Wagner PJ, Lam HMH. *J. Am. Chem. Soc.* 1980; 102:4167–4172.(b) Matsushita Y, Yamaguchi Y, Hikida T. *Chem. Phys.* 1996; 213:413–419.
63. Fukuzumi S, Ohkubo K. *J. Am. Chem. Soc.* 2002; 124:10270–10271. [PubMed: 12197716]
64. (a) Fukuzumi S, Tokuda Y, Kitano T, Okamoto T, Otera J. *J. Am. Chem. Soc.* 1993; 115:8960–8968. The KIE value is somewhat larger than those observed for proton-transfer reactions of ArCH_2^+ (KIE = 9-10) probably due to a larger contribution of the tunneling effect. (b) Ishikawa M, Fukuzumi S. *J. Chem. Soc., Faraday Trans. 1.* 1990; 86:3531–3536.(c) Fukuzumi S, Koumitsu S, Hironaka K, Tanaka T. *J. Am. Chem. Soc.* 1987; 109:305–316.

**Scheme 1.**

Formation of $(\text{TBP}_8\text{Cz})\text{Mn}^{\text{V}}(\text{O})$ from $(\text{TBP}_8\text{Cz})\text{Mn}^{\text{III}}$ with O_2 and Toluene Derivatives under Photoirradiation (White Light)

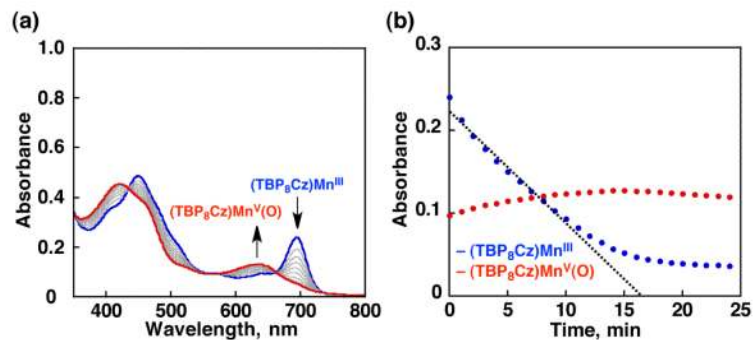


Figure 1. (a) UV-vis spectral changes and (b) time profiles of absorption changes at $\lambda = 695$ nm and 634 nm for the photochemical oxidation reaction of (TBP₈Cz)Mn^{III} (7.6×10^{-6} M) under irradiation (white light) in an aerobic solution of PhCN containing hexamethylbenzene (0.08 M) as a substrate at room temperature.

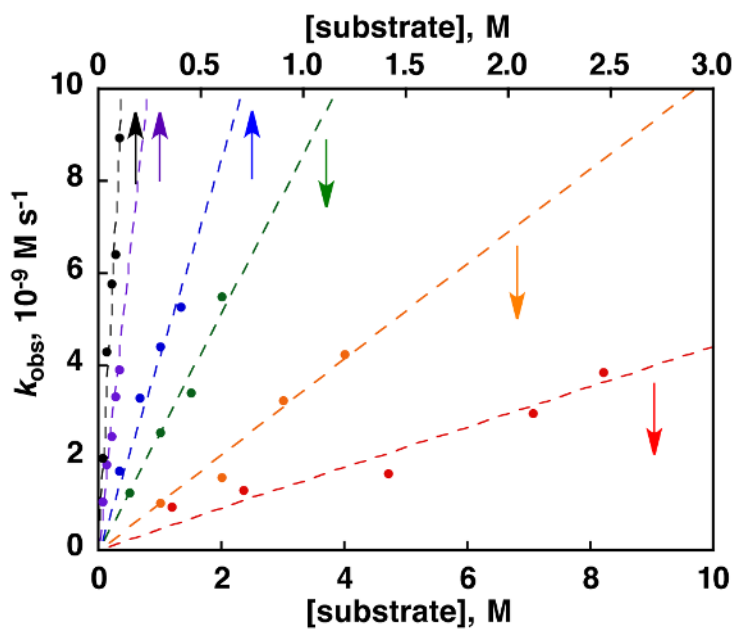


Figure 2. Plots of the observed zeroth-order rate constants (k_{obs}) of the oxidation reaction of $(\text{TBP}_8\text{Cz})\text{Mn}^{\text{III}}$ ($7.6 \times 10^{-6} \text{ M}$) under irradiation (white light) of an aerated PhCN solution containing toluene (red, 1.0 to 8.2 M), *p*-xylene (orange, 1.0 to 4.0 M), mesitylene (green, 0.5 to 2.0 M), durene (blue, 0.1 to 0.4 M), pentamethylbenzene (purple, 2.0×10^{-2} to $1.0 \times 10^{-1} \text{ M}$) or hexamethylbenzene (black, 2.0×10^{-2} to $1.0 \times 10^{-1} \text{ M}$) as a substrate at 298 K.

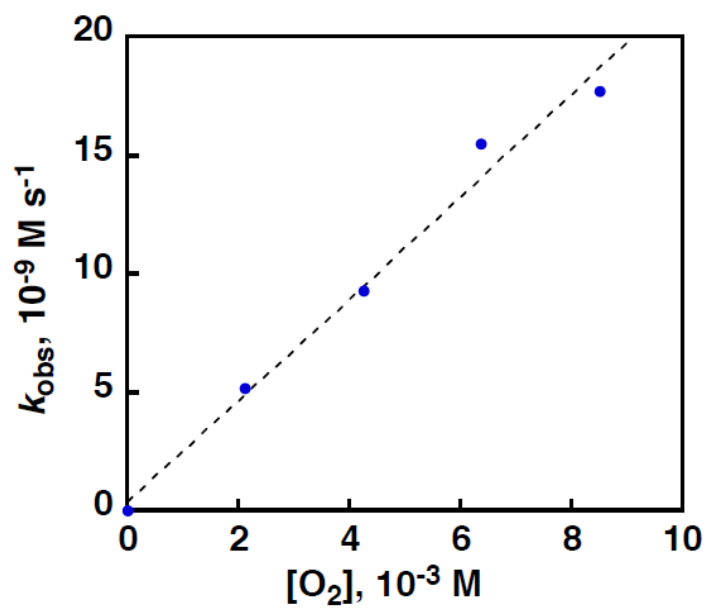


Figure 3. Plot of the observed zeroth-order rate constants (k_{obs}) for the oxidation of $(\text{TBP}_8\text{Cz})\text{Mn}^{\text{III}}$ ($7.6 \times 10^{-6} \text{ M}$) with O_2 and hexamethylbenzene (0.10 M) under photoirradiation M) (white light) in PhCN vs the oxygen concentration ($0 - 8.5 \times 10^{-3} \text{ M}$)³⁷ at 298 K.

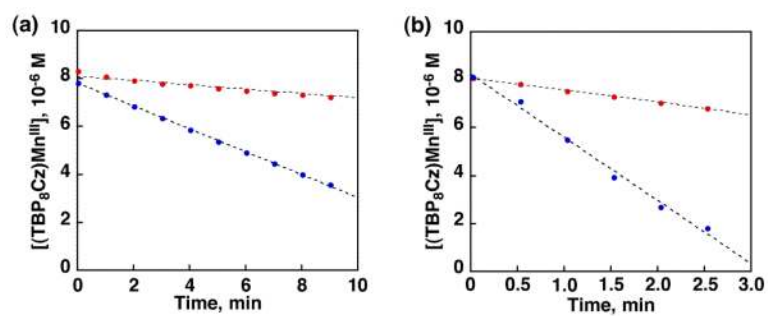


Figure 4. Time dependence of photochemical oxidation of $(\text{TBP}_8\text{Cz})\text{Mn}^{\text{III}}$ ($8.0 \times 10^{-6}\text{ M}$) with (a) M) $\text{C}_6\text{H}_5\text{CH}_3$ (blue, 2.0 M), $\text{C}_6\text{D}_5\text{CD}_3$ (red, 2.0 M), (b) mesitylene (blue, 2.0 M), or mesitylene- d_{12} (red, 2.0 M) under irradiation (white light) in O_2 -saturated PhCN at 298 K.

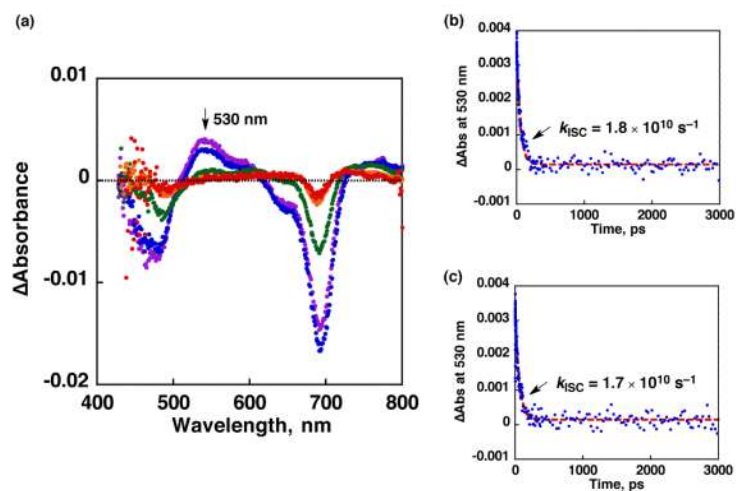


Figure 5.

(a) Transient absorbance spectral changes (purple after 1 ps, blue 10 ps, green 100 ps, III orange 1000 ps, and red 3000 ps) after photoexcitation of (TBP₈Cz)Mn in PhCN. Time profile of the generation and decay of [(TBP₈Cz)Mn^{III}]^{*} (⁵T) at $\lambda = 530$ nm under (b) N and (c) O. The -3 red lines are exponential fitting given in eqn (4) (see Experimental Section). $A_1 = 3.3 \times 10^{-4}$, $A_2 = 1.5 \times 10^{-4}$, and k (c).

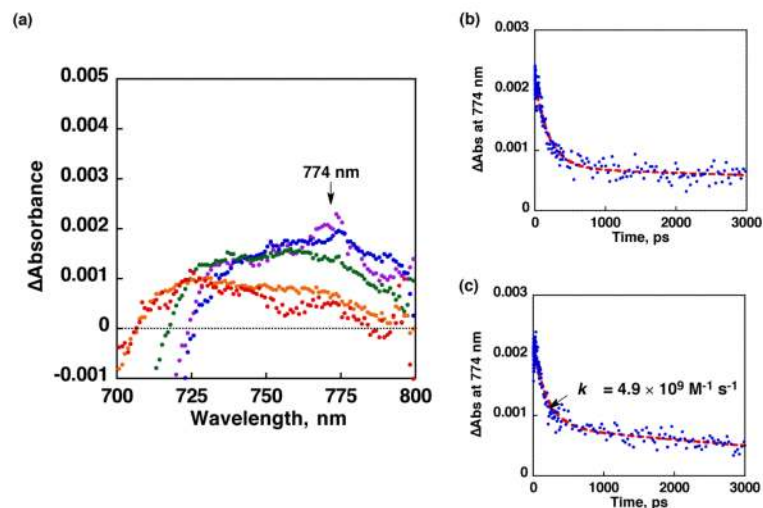
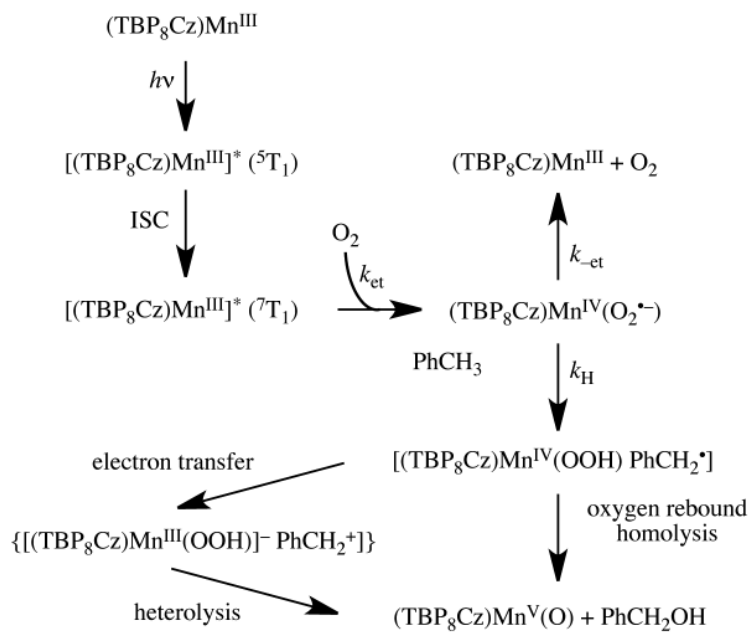
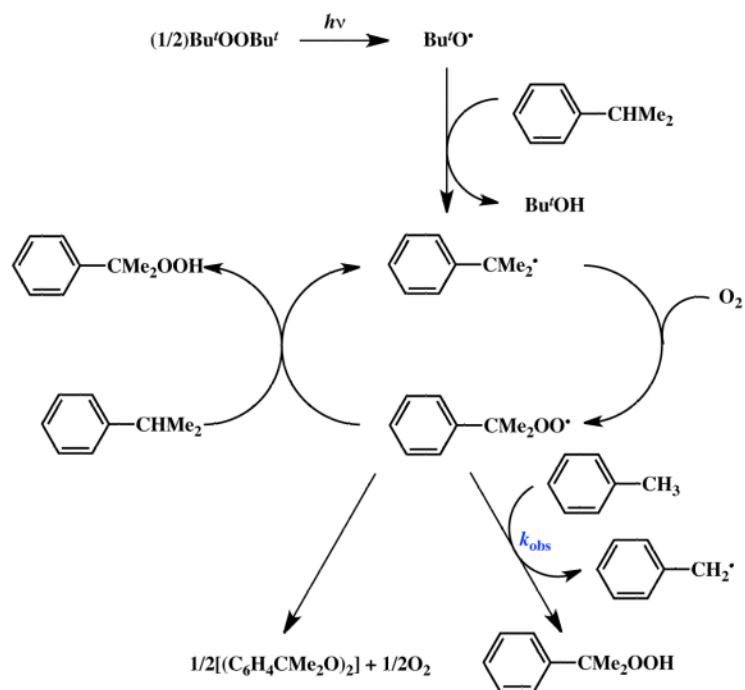


Figure 6. (a) Transient absorbance spectral changes (purple after 1 ps, blue 10 ps, green 100 ps, III orange 1000 ps, and red 3000 ps) after photoexcitation of $(\text{TBP}_8\text{Cz})\text{Mn}$ in PhCN. Decay time profiles of absorbance at 774 nm due to $[(\text{TBP}_8\text{Cz})\text{Mn}^{\text{III}}]^*$ (^7T) (b) in N-saturated PhCN and (c) in O_2 -saturated PhCN. Best-fit lines (red) obtained from a double-exponential kinetic model given in eqn (5) (see Experimental Section). $A_1 = 1.4 \times 10^{-3}$, $A_2 = 6.7 \times 10^{-3}$, $A_3 = 3.6 \times 10^{-3}$, $k_1 = 4.8 \times 10^9$, $k_2 = 6.3 \times 10^7$ for (b) and $A_1 = 1.0 \times 10^{-3}$, $A_2 = 1.1 \times 10^{-3}$, $A_3 = -4.5 \times 10^{-4}$, $k_1 = 5.0 \times 10^9$ and $k_2 = 1.1 \times 10^8$ for (c).



Scheme 2.
Mechanism of Photochemical Oxidation of (TBP₈Cz)Mn^{III} with O₂ and Toluene for Generation of (TBP₈Cz)Mn^V(O)



Scheme 3.
Generation of Cumylperoxyl Radical and Hydrogen Transfer from Toluene to $\text{PhCMe}_2\text{OO}^\bullet$ *

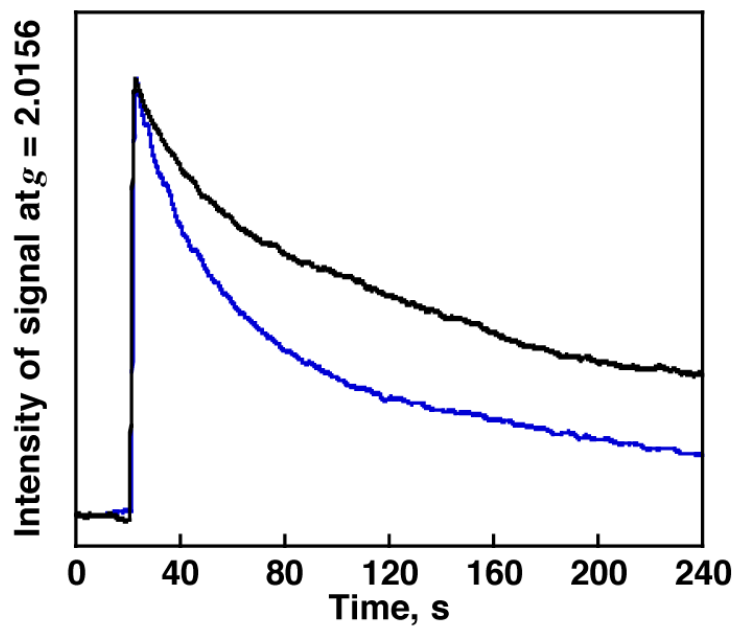


Figure 7. Time profiles of the EPR intensity change of cumylperoxyl radical in the absence (black line) and presence of toluene as a substrate (3 M, blue line) in aerated propionitrile at 193 K.

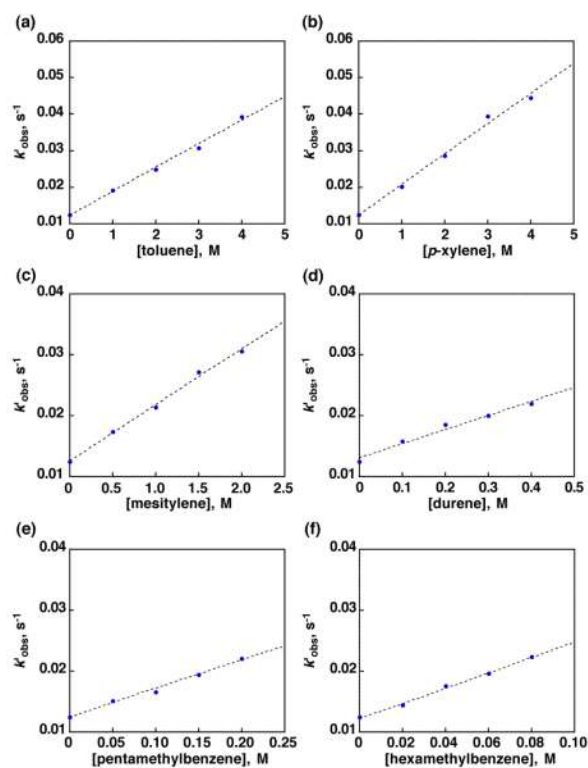


Figure 8. Plots of k'_{obs} vs concentrations of toluene derivatives for hydrogen-atom transfer from toluene derivatives to cumylperoxyl radical in aerated propionitrile at 193 K.

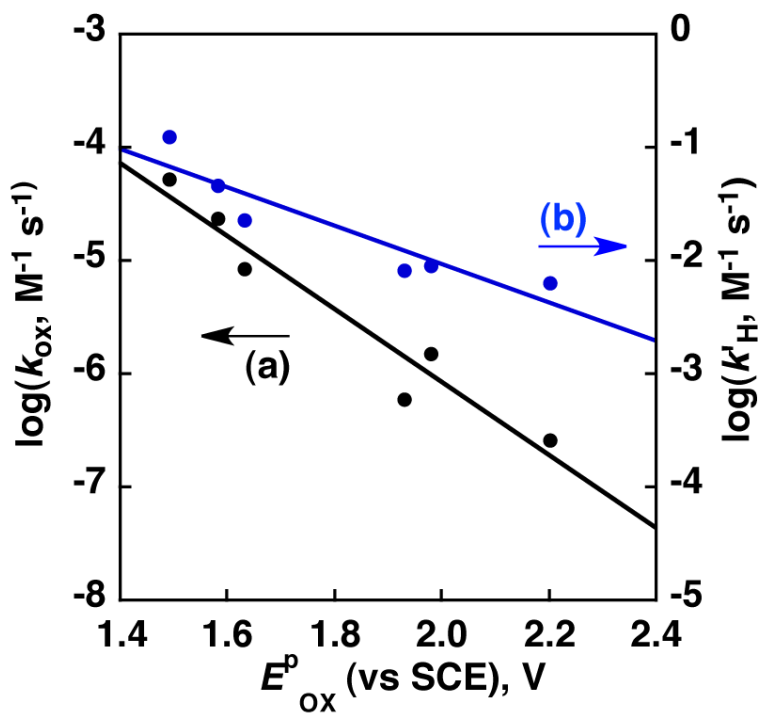


Figure 9. Plots of $\log k$ and $\log k'$ against the oxidation potential (E^p) of toluene derivatives III for hydrogen-atom transfer with (a) $(\text{TBP}_8\text{Cz})\text{Mn}$ and (b) cumylperoxyl radical.

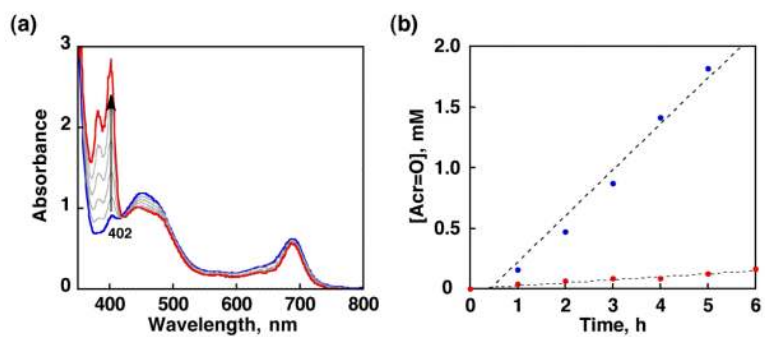
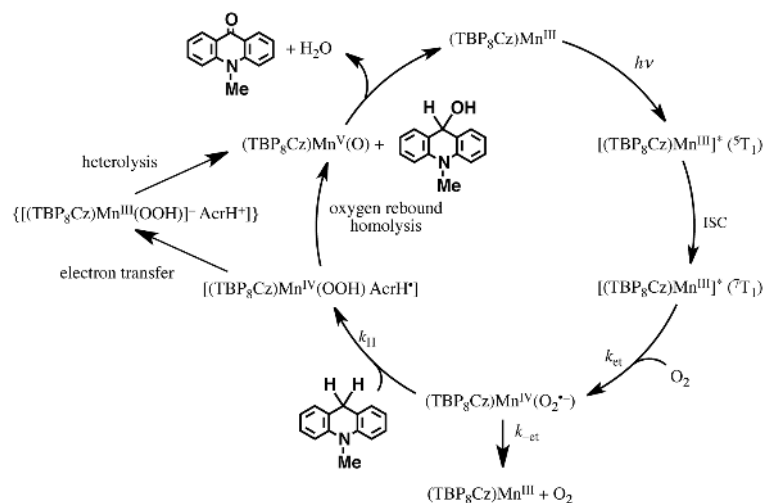


Figure 10.

(a) UV-vis spectral changes and (b) time course of formed Acr=O under III photoirradiation ($\lambda > 480$ nm) of an aerobic solution (0.5 mL) containing (TBP₈Cz)Mn (1.7×10^{-4} M) and AcrH (blue, 0.2 M) or AcrD₂ (red, 0.2 M).



Scheme 4.
Mechanism of Photocatalytic Reaction of $(\text{TBP}_8\text{Cz})\text{Mn}^{\text{III}}$ with O_2 and AcrH_2

Table 1

Second-Order Rate Constants for the Oxidation of (TBP₈Cz)Mn^{III} (k_{ox}) by O₂ with Toluene Derivatives in Aerated PhCN at 298 K and for the Hydrogen-Atom Transfer from Toluene Derivatives to Cumylperoxyl Radicals (k'_{H}) in Aerated Propionitrile at 193 K

substrate	$k_{\text{ox}}, \text{M}^{-1} \text{s}^{-1}$	$k'_{\text{H}}, \text{M}^{-1} \text{s}^{-1}$
toluene	$(4.0 \pm 0.4) \times 10^{-7}$	$(6.5 \pm 0.2) \times 10^{-3}$
<i>p</i> -xylene	$(1.1 \pm 0.3) \times 10^{-7}$	$(8.3 \pm 0.3) \times 10^{-3}$
mesitylene	$(2.7 \pm 0.1) \times 10^{-6}$	$(9.2 \pm 0.4) \times 10^{-3}$
durene	$(1.2 \pm 0.4) \times 10^{-6}$	$(2.3 \pm 0.1) \times 10^{-2}$
pentamethylbenzene	$(3.6 \pm 0.1) \times 10^{-5}$	$(4.7 \pm 0.2) \times 10^{-2}$
hexamethylbenzene	$(8.0 \pm 0.2) \times 10^{-5}$	$(1.3 \pm 0.1) \times 10^{-1}$